Failure Time Remapping in Compound Aftershock Sequences

Susanna Gross

January 1, 2003

Abstract

Compound aftershock sequences are of special interest because the decay of secondary aftershocks contains information about the mechanisms that generate all earthquakes. If earthquakes nucleate as a result of accelerating slip, growing cracks, or any similar failure process, then the rate of decay of aftershock sequences is a direct result of that failure process, as influenced by local material properties. The aftershocks are then triggered by the mainshock, moved closer to failure and concentrated on the curved part of loading curve, occurring earlier than they would have if the mainshock had not occurred. Secondary aftershocks, which are themselves triggered by an aftershock, are promoted towards failure twice, and consequently should decay differently than primary aftershocks do. The theory behind this concept is developed, explored with numerical models, and tested with a study of the aftershocks of the Hector Mine earthquake of 1999. Because the Hector Mine mainshock occurred during the aftershock sequence of the Landers 1992 earthquake, failure time re-mapping predicts a slightly different temporal distribution for the Hector Mine aftershocks than they would have had without the influence of the Landers mainshock. This prediction is testable. In this work three different types of aftershock decay relations are applied to 94 spatial subsets of aftershocks, and evaluated with two different statistical measures. Re-mapped aftershock decay models were superior for almost all the cases studied, regardless of the type of aftershock decay model used or the statistical measure. These results confirm previous work suggesting that the majority of aftershocks are not caused by their mainshock, only promoted toward failure, and most earthquakes nucleate through a failure process such as velocity dependent friction or stress corrosion cracking.

Introduction

One of the most interesting seismic phenomena is the occurrence of aftershocks. Large aftershocks trigger their own aftershock sequences, aftershocks here called secondary aftershocks, in order to distinguish them from the primary aftershocks triggered by the mainshock. An aftershock sequence is described as being compound when there is an obvious secondary aftershock sequence. The phenomenon of secondary aftershock sequences following large aftershocks has been recognized for a long time (Utsu, 1961) but only more recently have the aftershocks of smaller magnitude aftershocks been recognized. Lomnitz and Hax (1966) found no small scale clustering during aftershock sequences because of limitations of their data and analysis techniques. More recent studies have found significant clustering (e.g. Matcharashvili et al. 2000). Felzer et al. (2001) have constructed models that suggest most aftershocks are

secondary, in the sense that their most immediate trigger is another aftershock. Sornette and Sornette (1999) have shown that when secondary sequences generated by small magnitude aftershocks have an Omori decay, the decay of all the events together does not follow a simple Omori relationship, even though the sequence is not obviously compound. That result suggests that secondary aftershocks may not decay in the same way as primary aftershocks. Failure time re-mapping, the main topic of this paper, is a phenomenon which naturally produces secondary aftershocks that decay differently from primary aftershocks.

Currently there are several quite viable explanations for aftershock generation and decay, theories which ought to apply equally well to the failure process for all earthquakes. Our present difficulty is to choose among the theories, and select those which are valid for real seismogenic faults. Observations of aftershocks and in particular compound aftershock sequences can help distinguish between competing models of the earthquake failure process, which is the main reason they are interesting. All viable models of aftershock generation and decay involve some physical process which gives the aftershocks their temporal distribution. Some models imply that primary aftershocks are triggered through a process of failure time re-mapping, which means that their original times to failure as part of the background seismicity were changed by the mainshock, most likely as a result of the stress changes accompanying the mainshock (Stein, 1999, Belardinelli et al. 1999, Toda et al. 1998). The occurrence times of the secondary aftershocks would then be a result of doubly re-mapped failure times, and decay differently than the primary aftershocks. Other aftershock models (Hill et al. 1995, Lomnitz 1996, Gomberg 2001) do not involve re-mapping of occurrence times. The aftershocks could be "new" events, not any accelerated version of the background seismicity, in which case

we would expect the secondary aftershocks to decay much like the primary sequences do.

The implications of failure time re-mapping will be approached from several different directions in the work presented here. First the concept will be described and relevant equations will be developed and specialized for rate and state dependent friction models. Second, results of numerical simulations will be presented and modeled. Finally the new modeling techniques will be applied to aftershocks of the 1999 Hector Mine earthquake as influenced by the 1992 Landers stress step. Statistical tests are used to quantify how well the theory corresponds to observations.

Generalizing the Failure Process

Conceptual Description

When aftershocks occur through failure time re-mapping, the mainshock moves them forward in time, it does not generate new events. Essentially this means that there is some original temporal distribution of background seismicity that would have happened without the mainshock, and this distribution is altered as a result of the mainshock. The physical reasons why the failure times are changed vary from model to model, but the models all trigger aftershocks by altering the original distribution of failure times. The central point of this paper is that aftershocks triggered through failure time remapping decay in a way that reflects the original distribution of failure times, in addition to the remapping process. The physical process that promotes failure should not be influenced by the original distribution of failure times, but this means that the aftershocks it triggers will not always have the same temporal distribution. The most obvious real world example of the way the initial distribution of failure times changes the resulting aftershock distribution is the case of compound aftershock sequences. The sec-

ondary aftershocks in a compound sequence may be re-mapped in exactly the same way the primary aftershocks are, in the sense that a change in failure time for a given initial failure time and a given perturbation is the same. The difference is that the "initial" failure times of the secondary aftershocks are not the same as the initial failure times for the primary aftershocks. The distribution of failure times is altered twice, and therefore the doubly re-mapped secondary aftershocks decay differently than the singly re-mapped primary aftershocks do.

Failure Time Re-mapping Equations

The simplest way to represent failure time remapping is to write the remapping function R, which converts failure times of background earthquakes, t_b, to failure times of primary aftershocks t_p,

$$t_p = R(t_b). \qquad (1)$$

In this expression the mainshock occurs at $t = 0$, so R is defined only for positive values of its argument. Since R is only a function of the timing of the events, it can equally well be applied to the times of primary aftershocks, generating secondary aftershocks at times t_s following a secondary mainshock at t_2,

$$t_s - t_2 = R(t_p - t_2), \qquad (2)$$

which is very similar to the original expression, except for a time shift, starting the remapping at time t_2. Combining the last two equations,

$$t_s = R[R(t_b) - t_2] + t_2, \qquad (3)$$

we see how an event that would originally have occurred at t_b is doubly remapped, becoming a secondary aftershock that occurs at t_s.

In order to derive the observational consequences of the remapping, it is helpful to develop expressions for the distributions of the aftershock times we expect, assuming an initially uniform population of failure times t_b, producing a steady rate b of background events per unit time. Symbolically, this assumption can be written:

$$t_b \overset{d}{=} U, \qquad (4)$$

where U represents a uniform distribution. If we then apply the remapping function to both distributions,

$$R(t_b) \overset{d}{=} t_p \overset{d}{=} R(U) \qquad (5)$$

we have an expression for the distribution of primary aftershock times. This expression helps us to visualize the remapping function R, whose inverse is the cumulative event count curve, suitably scaled by the background rate. The distributions can be converted to cumulative event count curves $N(t)$, which are often used to quantify the decay of aftershocks. When we say that the background seismicity is uniformly distributed, we mean the the probability of an event occurring before some time T is

$$\Pr(t_b < T) = \frac{(t_b - t_{\min})}{b(t_{\max} - t_{\min})}. \qquad (6)$$

But $t_{\min}$ is generally zero, the time of the mainshock, the origin of the timescale is chosen there. When the background events are remapped to aftershock times t_p, the probability of an aftershock occurring before T is modified by the remapping function R:

$$\Pr(t_p < T) = \frac{R^{-1}(t_p)}{bt_{\max}}, \qquad (7)$$

which can be converted into a cumulative event count N through a change in units, multiplying by $bt_{\max}$,

3

$$N = bR^{-1}(t_p). \qquad (8)$$

If we rearrange this expression and recognize that $N = bt_b$,

$$R(N/b) = t_p, \qquad (9)$$

we recover the definition of the remapping function R, showing the consistency of this derivation.

Failure time remapping can occur as a result of several possible mechanisms, with velocity dependent friction being one. In this case, the slip velocity V of a fault patch increases toward failure, following a failure curve f, which is a function of time,

$$f(t) = \log(V). \qquad (10)$$

The failure curve f is responsible for generating aftershocks because it is curved on a semi-log plot (Figure 1), increasing in slope just before failure. Stress increases from the mainshock $\Delta\sigma_1$ produce increases in slip velocity that result in earlier failure times t_p, and concentrate the events on the curved part of the line, just before failure,

$$f(t_p) = f(t_b) + A\Delta\sigma_1, \qquad (11)$$

where $\Delta\sigma_1$ is the change in failure stress, incorporating both increases in shear stress and decreases in normal stress resolved onto the faults upon which the aftershocks occur, (e.g. Stein, 1999). $\Delta\sigma_1$ can also be negative, in which case it results in a seismicity decrease. Far from failure f has a constant slope, which means that the seismicity rate long after the mainshock is not changed by the remapping process. The function f can be related to the remapping function R by solving for primary aftershock times t_p,

$$t_p = f^{-1}(f(t_b) + A\Delta\sigma_1), \qquad (12)$$
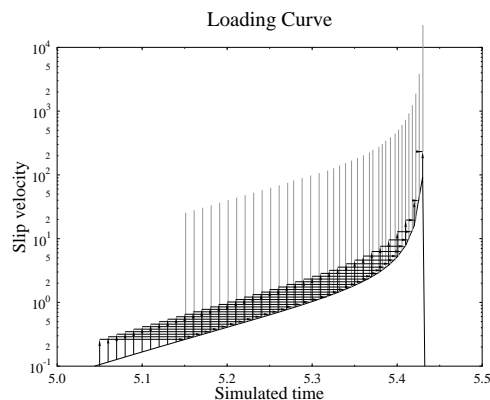
and then substituting for the lefthand side,

Figure 1: This figure illustrates the process of failure time remapping for a loading curve derived from Dieterich seismicity theory. The initial distribution of earthquake failure times is represented by the evenly spaced arrangement of black upward pointing arrows along the loading curve. The arrows all have the same length, because the response to the stress step they represent produces the same increment of log slip velocity on each nucleation site (all sites experience the same stress increment). The change in failure time that results is illustrated by horizontal arrows, which are not all the same length, because the time to failure represented by the new slip velocity is a function of the local slope of the loading curve. The bend in the loading curve concentrates the final slip velocities, (represented by vertical grey line segments) and produces the primary aftershock sequence.

4

$$R(t_b) = f^{-1}(f(t_b) + A\Delta\sigma_1). \qquad (13)$$

In order to see how secondary aftershocks occurring on a fault with velocity dependent friction are distributed in time, the remapping can be applied to the primary aftershocks,

$$t_s = t_2 + f^{-1}(f(t_p) + A\Delta\sigma_2 - t_2), \qquad (14)$$

and the expression rearranged,

$$f(t_s - t_2) = f(t_p) + A\Delta\sigma_2 - t_2, \qquad (15)$$

making it easier to substitute in the relationship between primary aftershocks and background seismicity:

$$f(t_s - t_2) = f(t_b) + A\Delta\sigma_1 + A\Delta\sigma_2 - t_2, \quad (16)$$

which makes it clear that the effect of an immediate secondary mainshock is to change the number of aftershocks without altering their temporal distribution. Only when t_2 is nonzero is there a difference between the decay relations that apply to secondary aftershocks as contrasted with primary aftershocks. Far from failure the f function produces a linear increase of $\log V$ with t, so all events are moved toward or away failure by the same amount, and there is no change in seismicity rate. Even though the timing of events far from failure has been altered, their rate is unchanged, and so we do not ordinarily call these events aftershocks. The population of slip velocities only retains evidence of a mainshock as long as the seismicity rate is altered, which is a length of time equal to the width of the curved portion of the failure curve. Secondary aftershocks are moved twice along the failure curve, but they will not decay differently than primary aftershocks unless both times the remapping involved a change in rate of seismicity, movement toward or away from the curved part of the failure curve.

Aftershock models

The three main aftershock models used in this work were modified Omori, Dieterich, and stretched exponential. The modified Omori relation (Utsu 1961) with an additional background term (Gross and Kisslinger 1994) is

$$n(t) = \frac{K}{(t+c)^p} + b. \qquad (17)$$

Variations on modified Omori include Modified Omori with adjustable background (MOMb), Modified Omori with fixed background (MOMB), and Modified Omori with no free parameters (MOMF). The fixed background in MOMB models is computed from the observed rate of background events before the first mainshock. The fixed modified Omori model uses that same fixed background, and gets the c and p-values from a fit to the entire data set.

The Dieterich (1994) model may be written,

$$n(t) = \frac{b}{\left[\exp\left(\frac{-\Delta\sigma_F}{A_D\sigma}\right) - 1\right]\exp\frac{-t}{t_a} + 1}, \qquad (18)$$

which was derived using equations developed to describe laboratory observations of rate and state dependent friction.

The stretched exponential,

$$n(t) = qN^*(0)\frac{1}{t}\left(\frac{t}{t_0}\right)^q \exp[-\left(\frac{t}{t_0}\right)^q] + b, \quad (19)$$

was first proposed by Carl Kisslinger (1993), and is usually fit with a background term b (STREXPb).

In equations 17-19 $n(t)$ is the number of events occurring per unit time, at time t. The K parameter in the original modified Omori function and $N^*(0)$ in the stretched exponential are related to the total number of aftershocks in the sequence, and can be computed directly from the observed number of

events and the other parameters. In the Dieterich aftershock decay function (6) the number of aftershocks is proportional to the background rate b and increases with increasing failure stress step $\Delta\sigma_F$, as scaled by the velocity effect constant A_D and the normal stress σ. The only other parameter in the Dieterich decay relation is t_a, the duration of the aftershock sequence. The Dieterich decay relation resembles a modified Omori sequence with decay power $p = 1$ at times less than t_a but greater than time it starts to decay. The time the Dieterich relation starts decaying, analogous to c in the modified Omori relation, decreases with increasing stress step $\Delta\sigma_F$. For the stretched exponential, t_0 controls the transition from power law decay (with a power q) and exponential decay.

Aftershock decay modeling

A method for fitting the Dieterich decay relation to the temporal decay of the aftershocks is needed in order to select the best-fitting models and test failure time re-mapping. A practical technique for fitting and comparing aftershock models having a variety of functional forms has been developed (Gross, 1996; Gross and Kisslinger, 1994; Kisslinger, 1993; Ogata 1983). This technique finds the best-fitting model by minimizing the Akaike information criterion (AIC), which also minimizes the difference between the best fitting model and the unknown true model.

For an aftershock model having n_p free parameters and a modeled rate $n(t_i)$, as a function of the time of the ith aftershock, the AIC is

$$\text{AIC} = 2N - 2\sum_{i=1}^{N}\log(n(t_i)) + 2n_p, \qquad (20)$$

where N is the total number of aftershocks observed. By minimizing the AIC over the possible

models, we maximize the model rates n at the times of events t_i. The three models fit in this work (equations (17), (18) and (19)) have $n_p = 3$ free parameters, K, c and p for the Modified Omori model, q, N_0 and and t_0 for the stretched exponential and t_a, b and $-\Delta\sigma_F/A_D\sigma$ for the Dieterich model. In order to include background activity an additional parameter b is usually employed in fitting the Modified Omori and stretched exponential. The minimization is carried out by using the technique described by Gross (1996). The lowest minimum from a series of 20 downhill simplex runs is selected, with each run started from a different, randomly selected set of initial parameters. The last 10 runs are started progressively closer to the best value found up to that point.

Modeling Compound Sequences

To fit models to compound aftershock sequences with re-mapped failure times it is only necessary to apply a conventional aftershock model twice. The primary mainshock and its aftershocks are fit using some standard technique which permits the expected cumulative number of events at the time of each aftershock to be evaluated. Then the model is extrapolated to the times of all the secondary aftershocks. The cumulative number of events in a model of an aftershock sequence may be treated as a time, called Frequency Linearized Time (Ogata and Shimazaki, 1984)

$$FLT \equiv \int_{t=0}^{T} n(t)dt. \qquad (21)$$

When this quantity is graphed as a function of the observed number of events, the decay of the primary aftershock sequence is gone, and the secondary sequence appears as if it occurred in isolation. This is illustrated in figures 2 and 3.

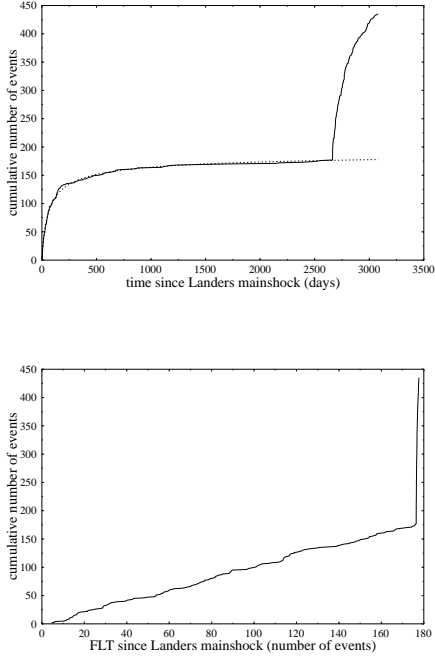The transformation of the time axis which occurs when we plot frequency linearized time is the same

Figure 2: These curves show the cumulative number of events that occurred within a 64 km box near Landers and Hector Mine aftershock zones. The dashed curve is a fit to the Landers aftershocks extrapolated through the Hector sequence. When the time scale is transformed to Frequency Linearized Time (bottom panel) the first aftershock sequence (Landers) is flattened away, and appears as if it were background seismicity. This also changes the shape of the secondary sequence (Hector Mine), but it is difficult to see the new shape because the new time scale is so compressed.

transformation of failure time that the secondary aftershocks undergo as a result of the primary mainshock. So the secondary sequence may be fit just as if it were primary, using the same techniques developed for simple aftershock sequences. Transformation to frequency linearized time is the modeling technique used to fit secondary re-mapped aftershocks in this work. In order to evaluate the goodness of fit using the AIC or likelihood, it is necessary to transform back to physical time from frequency linearized time.
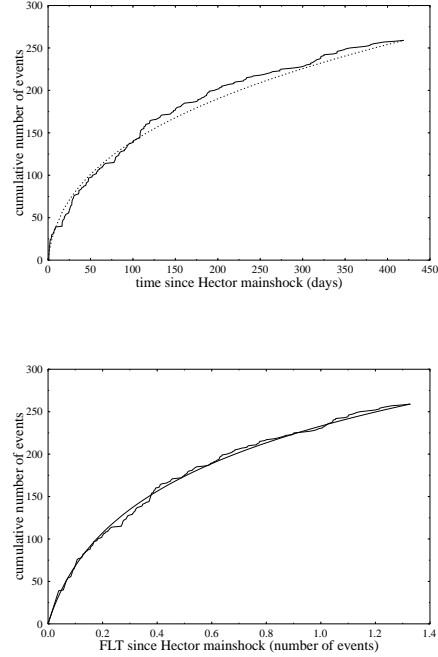
Figure 3: This pair of figures shows the same data and the same Modified Omori model as in the previous figure, but new constraints have been placed on the time scale, so the change in shape of the secondary sequence (Hector Mine) is now visible. The dashed curve in this case is a Modified Omori fit to the Hector aftershocks. Transformation to Frequency Linearized Time improves the fit.

Numerical Simulations

In order to verify the failure time re-mapping process and the effect it has upon secondary aftershocks, I constructed a simple numerical model of earthquake nucleation on a population of faults that obey rate and state dependent friction. This model marches forward in time at a steady rate, applying a given stress history to all of the faults. The faults have state variables θ_i and velocities V, which are updated in sequence at each time step given the current shear stress τ and normal stress σ,

7

$$\tau = \sigma[\mu_0 + A\ln(V/V^*) + B\ln(\theta/\theta^*)] \qquad (22)$$

$$d\theta = [1/V - \theta/D_c]V\,dt - [\frac{\alpha\theta}{B\sigma}]d\sigma, \qquad (23)$$

but there is no stress transfer between faults. Although these equations can be written for multiple state variables B_i, α_i, θ_i and D_{ci}, the cases presented here were computed with a single set of state variables. When the slip velocity of a fault reaches $1000V^* = 10$ cm/day it is declared to have ruptured, and its velocity is reset to $1 \times 10^{-10}V^*$. At failure the stress drop on the fault is set equal to the current stress value, reflecting an assumption of zero residual stress. This permits the residual stress to cycle upward again as the velocity gradually increases to the failure threshold. The number of faults that rupture in each time step of the model is output, and may be compared with small magnitude natural seismic activity. The model is not meant to represent the full complexity of real fault nucleation, and neglects momentum as well as stress transfer between the fault patches, but it includes variations in the frictional properties A, the direct velocity effect, B which weights the effect of the state variables, and D_c the critical slip distance. There are also variations in the initial state variables and in the stresses, but the particular values chosen are not important. The model is run through many cycles of failure at a steady rate of loading. The velocities and state variables reach an equilibrium, simulating the conditions which generate a steady rate of background seismicity before the stress step from a mainshock perturbs the state variables to generate the aftershocks.

In order to test the numerical model, I first see if it can reproduce the theoretical results derived for a population of faults having friction that obeys rate and state dependent friction. Dieterich (1994) developed these equations for the case of a single step
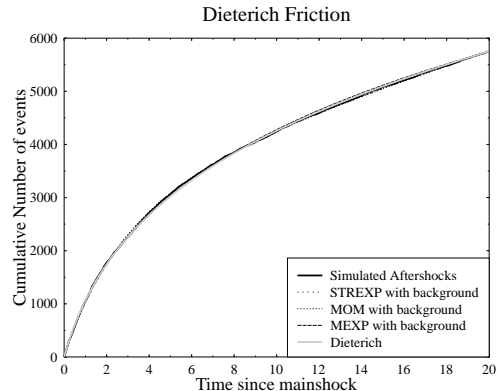

Figure 4: This synthetic aftershock sequence was generated using a numerical model which had been allowed to equilibrate for a long time without a mainshock beforehand. The sequence is best fit with a Dieterich aftershock model.

in stress. Figure 4 shows a synthetic aftershock sequence generated by a model run with 100,000 faults, $\mu_0 = 0.5$, just a single state variable, with B uniformly distributed from .008 to .016, and D_c uniformly distributed from .0625 to .125 m. The background loading was steady at a rate of 100 Pa/day, and lasted for 10^5 days or 273 years before a stress step of 4×10^5 Pa was applied to generate aftershocks.

As Figure 4 shows, we find that the numerical model produces aftershock sequences that decay as predicted by Dieterich seismicity theory. Several other aftershock decay models are also plotted on the graph, and they all match the data quite well. The Dieterich model fits best because it has the best Akaike Information Criterion ($\Delta AIC = 0.5$) when compared to the most successful other model, Modified Omori with background. This confirms that the model adequately represents Dieterich seismicity theory.

8

The model was also tested by generating a sequence with known parameters, and seeing if they can be recovered from the best-fitting parameter values. In this case
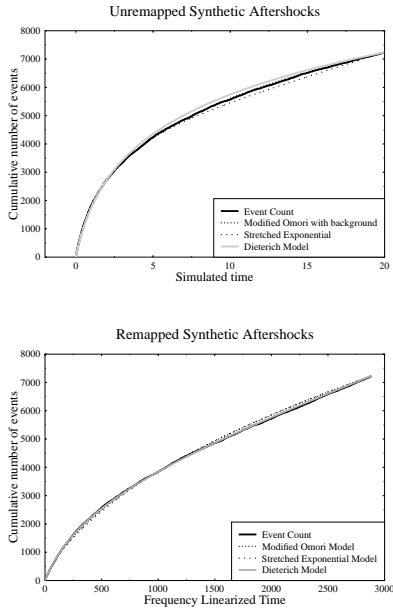

Figure 5: This synthetic secondary sequence is shown without failure time remapping (top panel) and with failure time remapping (bottom panel). The remapping improves the fit of aftershock decay models, especially the Dieterich decay relation, which applies to these data because they were generated using Dietrich friction.

$$t_a = A_D \sigma / \dot{\sigma}_F, \qquad (24)$$

t_a should be 1000 days. Correcting for the inaccuracy of the background rate of seismicity, b estimated from the aftershock sequence,:

$$
\begin{aligned}
t_a &= \frac{31.3 \text{ days}}{(2 \text{ events/day})} \times 59.3 \ \frac{\text{events}}{\text{day}} \quad (25) \\
&= 928 \text{ days},
\end{aligned}
$$

which is gratifyingly close to the theoretically expected value of 1000 days.

The more complicated case of two stress steps applied to the numerical model produces a realistic-looking compound sequence. As Dieterich (1994) explains, the sequences still have the characteristic $1/t$ decay at intermediate times, but there are some interesting effects at shorter times not discussed there. The secondary sequence decays differently at first because of the doubly-remapped failure times the early aftershocks have. Secondary aftershocks resulting from a sufficiently large secondary stress step will not show this effect because all the remaining primary aftershocks occur at the same time as the secondary mainshock.

Fitting the secondary aftershocks with aftershock decay models without re-mapping results in considerable misfit (top panel of Figure 5) but when the primary aftershock sequence is reduced to a straight line by plotting cumulative number versus frequency linearized time (equation 9), the secondary aftershocks are better modeled. In particular, the Dieterich aftershock model is improved, and it provides the best fit ($\Delta AIC = 27$) when compared with the Modified Omori model with background, the second-best model.

Application to Hector Mine

There are innumerable tests of the failure time remapping concept we could construct using real data, but the best ones involve large numbers of aftershocks, so that the results are clear, and well defined mainshock sources, so that the calculation of stress transfer is reasonably well constrained. The 1999 Hector Mine earthquake was chosen as a secondary mainshock because it follows the well-studied 1992 Landers earthquake, occurred in a very well monitored part of the world, and the aftershock zones

overlap.

The catalog of seismicity used in this work was compiled by the Caltech USGS southern California seismic network, beginning in January 1981 and ending in December 2000. The minimum magnitude used was $M_L \geq 2.0$ but no spatial cut was applied. The catalog was divided into a spatial grid of boxes (Figure 6) whose sizes reflect the level of seismic activity. The pattern of boxes shown in figure 6 was created with an automatic clustering algorithm that divides seismicity into compact subsets according to activity level. The algorithm starts with a 1 km grid of possible clusters, and compares the number of events in each cube with a minimum count, in this case 300 events. Any cubes that meet this threshold are saved, and their events excluded from larger scale clusters. Then the resolution of the grid is halved, defining a regular network of 2km cubes. The 2km seismicity counts are compared with the same threshold, qualifying data saved, and aggregated again. The process ends when the maximum permitted cluster size is reached, in this case 64 km, and all remaining events are assigned to cubes which may not meet the threshold. The algorithm groups the data by location so that quantities which vary with location can be studied in relatively homogeneous subsets. Dividing the data up by location also provides a relatively large number of cases to test, and segregates influences that make the tests dependent upon one another as much as possible.

In order to test the failure time re-mapping hypothesis I fit a variety of aftershock decay models to the subsets just discussed, using two different statistical measures to define the quality of the fit. The first measure is the Kolmogorov-Smirnov statistic, which is defined to be the greatest difference between the cumulative distribution functions being compared. The better the fit, the smaller the value, which can range between zero and 1. The second test is an evaluation of log-likelihood, the same method used

Table 2: Log Likelihoods of Hector Aftershocks

Model	np	sequential	remapped	ΔL
strexpb	4	-275	-245	+30
momb	4	-260	-237	+23
momB	3	-264	-255	+9
dieterich	3	-269	-253	+16
momF	0	-319	-322	-3

These average log likelihoods are less negative when the probability of the observed data is greater. Therefore the best-fitting models are those with the least negative log-likelihoods, and the fewest parameters, np. Each parameter should improve the fit by a factor of $2 \times e$, which means two units should be added to the momB and dieterich log likelihoods when comparing with the stretched exponential or momb log likelihoods. The best-fitting models in this table are the modified Omori and stretched exponential decays, both with failure time re-mapping.

to evaluate the goodness of fit when modeling individual aftershock sequences. In this application the cumulative distribution functions are actually a cumulative event count as a function of time, normalized to the total number of events. In each case the primary and secondary sequences were fit independently, using a maximum likelihood technique, and then the compound sequence was reassembled and evaluated using the KS statistic, in Table 1, or the maximum likelihood statistic, as in Table 2. Only sequences with at least 10 secondary aftershocks were used in the computation of the K-S shown in Table 1.

I fit the re-mapped secondary aftershocks by extrapolating the best fitting primary sequence and transforming to Frequency Linearized time as discussed in the section on modeling compound sequences. The re-mapped fits were compared to fits made without any remapping. This comparison was made for 94 subsets, eliminating those which had fewer than 50 events following the Landers mainshock.
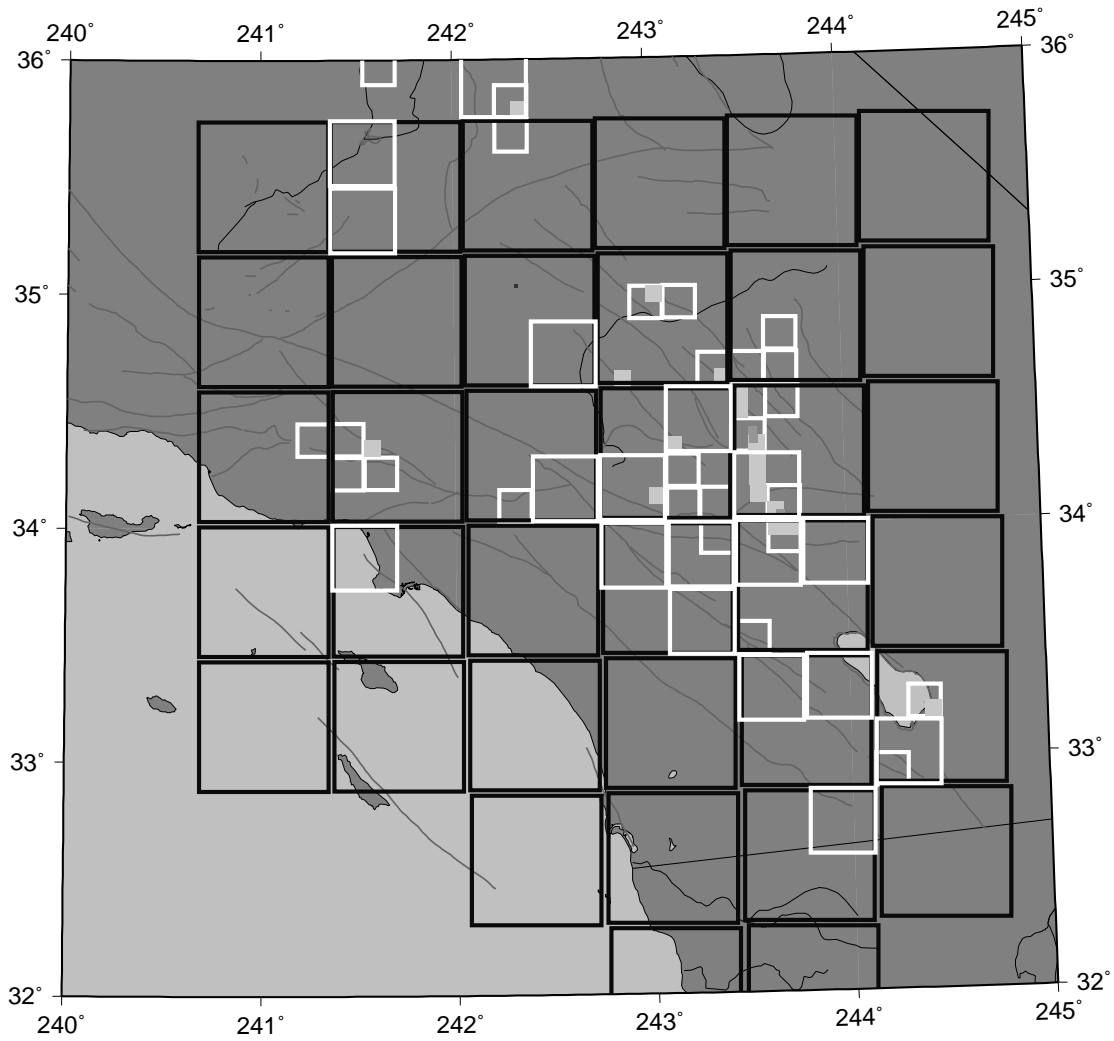
10

Subsets

Figure 6: These cubes define the spatial subsets used to analyze seismicity for the failure time re-mapping fits. They are defined in a hierarchy of sizes, from 64 km to 1 km, with their range of depths equal to their horizontal extent. When they overlap the smaller sizes take precedence over the larger, so events are assigned to the smallest cube that encloses their hypocenter.

Table 1: KS statistics of Hector Aftershock Fits

	MOMb	MOMB	Strexpb	MOMF	Dieterich
Sequential	.13	.13	.13	.20	.13
Re-mapped	.10	.12	.09	.30	.10

These Kolmogorov-Smirnov statistics are a measure of misfit, with smaller values corresponding to better fits. The 5 different models were applied to subsets of Hector aftershocks with either sequential (unremapped) sequences or re-mapped sequences taken from the decay of the Landers aftershocks for the same region. The best model is Stretched Exponential, followed by Modified Omori and Dieterich, all including failure time re-mapping.

Discussion

The results presented here support the applicability of failure time re-mapping to both modeled and observed aftershocks. This is particularly easy to show for the case of simulated events, because the data sets can be made as large and uniform as desired, and so the statistical uncertainties are minimal. With real data there is more uncertainty about the statistics, but far less uncertainty about the relevance of the result. In the case of Hector Mine, it does appear that most aftershocks have been generated by some process that involves a re-mapping of failure times, as both statistical tests show significantly better fits when the sequences are re-mapped before being fit.

Dividing the aftershocks into spatial subsets seems to have given the stretched exponential and Dieterich aftershock decay relations an advantage compared to the more usual situation when aftershocks from various locations are blended together. The blending could easily mask the rather subtle differences between decay relations, especially when variations in stress step are responsible for variations in the decay relation, and stress step varies with location.

Conclusions

(1) Failure processes which generate aftershocks by advancing the failure times of background events will generate secondary aftershocks that decay differently than the primary aftershocks do.

(2) Secondary aftershocks may be fit by transforming time to frequency linearized time $FLT(t)$ to remove the primary aftershock sequence.

(3) Aftershocks of the 1999 Hector Mine earthquake show this effect when grouped into subsets based upon location. Remapped aftershock decay models provide a better fit to these data.

(4) Although these results do not rule out the generation of some "new" events in aftershock sequences, they suggest most events are triggered by some mechanism that involves the acceleration of background seismicity, such as time dependent friction or stress corrosion cracking.

representing the official policies, either expressed or implied, of the U.S. Government.

References

Belardinelli, M.E., M. Cocco, O. Coutant and F. Cotton, (1999), Redistribution of dynamic stress during coseismic ruptures: Evidence for fault interaction and earthquake triggering, *J. Geophys. Res.*, *104*, 14925-14945.

Dieterich, J. H., (1994), A constitutive law for rate of earthquake production and its application to earthquake clustering, *J. Geophys. Res.*, *99*, 2601-2618.

Felzer, K. R., T. W. Becker, R. E. Abercrombie, G. Ekström and J. R. Rice, (2001), Aftershocks can significantly alter stress change patterns produced by their mainshock, *Eos Trans. AGU*, *82(47),* Fall Meet. Suppl., Abstract S11C-11.

Gomberg, J., (2001) The failure of earthquake failure models, *J. Geophys. Res.*, *106*, 16253-16263.

Gross, S. J., (1996), Aftershocks of nuclear explosions compared to natural aftershocks, *Bull. Seismol. Soc. Am.*, *86*, 1054-1060.

Gross, S. J., and C. Kisslinger, (1994), Tests of models of aftershock rate decay, *Bull. Seismol. Soc. Am. 84*, 1571-1579.

Hill, D. P., M. J. S. Johnston, J. O Langbein and R. Bilham, (1995), Response of Long Valley caldera to the M_w = 7.3 Landers, California, earthquake, *J. Geophys. Res.*, *100*, 12985-13005.

Kisslinger, C., (1993), The stretched exponential function as an alternative model for aftershock decay rate, *J. Geophys. Res.*, *98*, 1913-1922.

Lomnitz, C., (1996), Search of a worldwide catalog for earthquakes triggered at intermediate distances, *Bull. Seismol. Soc. Am. 86*, 293-298.

Lomnitz, C. and A. Hax, (1966), Clustering in aftershock sequences, in AGU monograph 10 *The Earth Beneath the Continents*, 502-508.

Matcharashvili, T., T. Chelidze, Z. Javakhishvili (2000), Nonlinear analysis of magnitude and interevent time interval sequences for earthquakes of the Caucasian region, *Nonlinear Processes in Geophysics* 7(1-2), 9-19.

Ogata, Y., (1983), Estimation of the parameters in the modified Omori formula for aftershock sequences by the maximum likelihood procedure, *J. Phys. Earth*, *31*, 115-124.

Ogata, Y. and K. Shimazaki (1984), Transition from aftershock to normal activity: The 1965 Rat Islands earthquake aftershock sequence, *Bull. Seismol. Soc. Am.*, **74**, 1757-1765.

Sornette, A. and D. Sornette, (1999) Renormalization of earthquake aftershocks, *Geophys. Res. Lett.*, *26*, 1981-1984.

Stein, Ross S., (1999), The role of stress transfer in earthquake occurrence, *Nature*, **402**, 605-609.

Toda, Shinji, Ross S. Stein, Paul A. Reasenberg, James H. Dieterich and Akio Yoshida, (1998), Stress transferred by the 1995 M_w = 6.9 Kobe, Japan, shock: Effect on aftershocks and future earthquake probabilities, *J. Geophys. Res.*, *103*, 24543-24565.

Utsu, T., (1961), A statistical study on the occurrence of aftershocks, *Geophys. Mag.*, **30**, 521-605.

Author Affiliation

Susanna Gross sjg@colorado.edu Cooperative Institute for Research in the Environmental Sciences University of Colorado at Boulder 216 UCB, Boulder, CO 80309